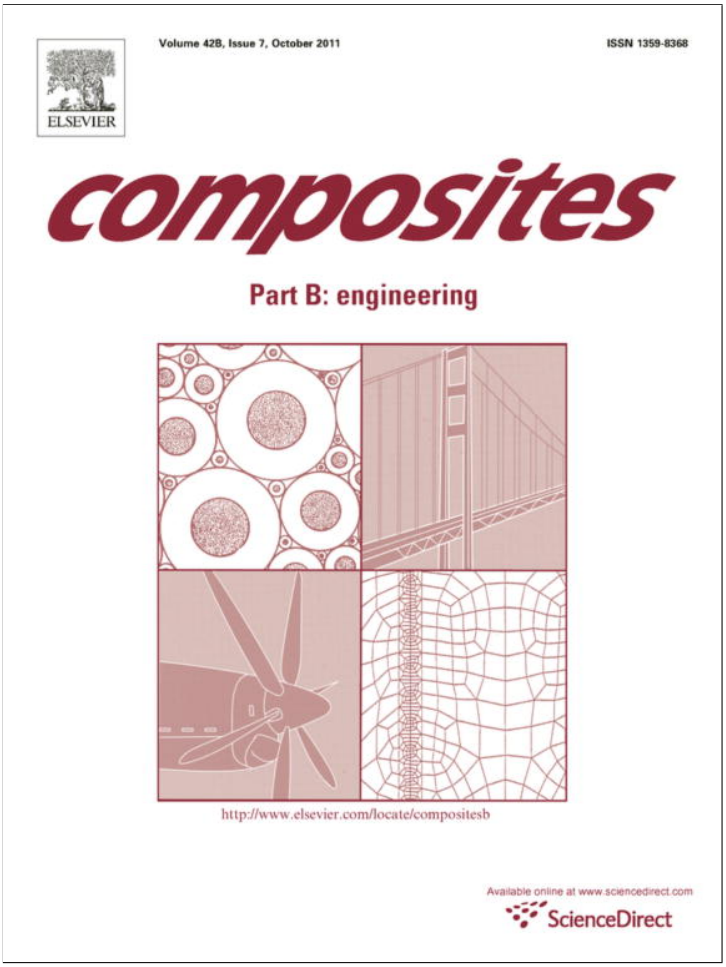

Composites: Part B 42 (2011) 1920–1928

Contents lists available at ScienceDirect

Composites: Part B

journal homepage: www.elsevier.com/locate/compositesb

# Mechanical response of PHB- and cellulose acetate natural fiber-reinforced composites for construction applications

S.J. Christian [a], S.L. Billington [b,*]

[a] Department of Civil and Environmental Engineering, Carnegie Mellon University, Pittsburgh, PA 15213-3890, United States
[b] Department of Civil and Environmental Engineering, Stanford University, Stanford, CA 94305-4020, United States

ARTICLE INFO

*Article history:*
Received 3 February 2011
Received in revised form 14 May 2011
Accepted 30 May 2011
Available online 6 June 2011

*Keywords:*
A. Polymer–matrix composites
B. Mechanical properties
C. Laminate mechanics
E. Lay-up (manual)
Biobased composite

ABSTRACT

Biobased composites are being evaluated for construction applications where wood or petroleum-based composites are currently used. The biobased composites studied are made from biopolymers and plant-based fibers and have been demonstrated to rapidly biodegrade in anaerobic conditions to methane thereby reducing construction-related landfill waste and producing a useful end product, namely fuel for energy or feedstock to grow more biopolymer. Mechanical properties are evaluated for hemp fabric/cellulose acetate and hemp fabric/poly(hydroxybutyrate) (PHB) composites. The composites have comparable strength to structural lumber and engineered wood products, with stiffness comparable to most engineered wood products. Classical laminate plate theory sufficiently predicts initial laminate behavior from ply-level experimental data. Simple nonlinear models using laminate plate theory and uncoupled ply-level experimental constitutive response are evaluated.



## 1. Introduction

Biobased composite materials comprised of a biobased polymer and natural plant-based fibers, are being investigated for use in construction applications with the aim of reducing the negative environmental impacts of construction materials. In 2003, 170 million tons of construction and demolition debris was generated with an estimated 52% of the debris disposed in landfills [1]. Construction and demolition debris is composed of 30–50% wood, drywall, and plastic [2]. These materials are generally recalcitrant in landfills and can potentially be replaced by biobased composite materials that can more rapidly biodegrade. In an anaerobic landfill environment, biobased composite materials can biodegrade to produce biogas including methane, which may be captured and sold as a fuel or used as a feedstock to produce a new generation of some biopolymers. A closed-loop life-cycle is envisioned for these materials wherein their degradation products are used to generate new polymer, which in turn may be combined with plant fibers to make a new generation of composites.

Two biobased composites are studied here. Both composites use hemp fiber fabric as reinforcement, in one case reinforcing a cellulose acetate matrix, derived from plants, and in another reinforcing a poly(hydroxybutyrate) (PHB) matrix, derived by bacterial fermentation. The mechanical response of these materials is measured and assessed for potential use in construction applications by comparing measured properties to wood and wood-based materials. The ability of established models to predict composite properties from constituent properties and to predict laminate behavior from ply-level behavior are assessed as potential tools for designing biobased composite materials for construction applications.

## 2. Background

Significant research has been conducted in recent years on biobased composites (see for example, [3–5]) with some attention given to potential construction applications of the materials. Most research and development on biobased composites targets the packaging, automobile, medical, and interior design industries [6,7]. Building-related natural-fiber composite research has primarily focused on petroleum-derived (or partially petroleum-derived) polymers [e.g., 8–15]. Very little research has been conducted on fully biobased polymer natural fiber composites for construction-related applications as studied here.

Short-hemp fiber/cellulose acetate composites [16,17] suggest that this fully biobased combination of materials produces behavior appropriate for use in construction. PHB and various co-polymers of PHB combined with hemp [18,19], flax [20–22], jute [23,24], bamboo [25], abaca [26], and pineapple leaf fibers [27] also show promise for use in construction. Textile fabrics have been investigated and observed to provide multi-dimensional properties [5,24,28,29] and are the focus of this research for their potential for building applications.

* Corresponding author. Tel.: +1 650 723 4125; fax: +1 650 723 7514.
*E-mail address:* billington@stanford.edu (S.L. Billington).

1359-8368/$ - see front matter © 2011 Elsevier Ltd. All rights reserved.
doi:10.1016/j.compositesb.2011.05.039

Mechanical modeling of biobased composite materials mostly has been limited to micromechanical modeling of short-fiber biobased composites with empirical modifications generally necessary. Micromechanical models have been applied to a limited extent to continuous fiber composites [10]. At the structural scale, basic mechanics has been used to predict flexural behavior from ply behavior in a biobased composite sandwich component [30], and cellular cross-sections made from short fiber composites were modeled as homogeneous materials using finite element modeling [31].

Laminate behavior has not been evaluated for biobased composites and is presented herein. A combination of classical laminate plate theory (CLPT) and nonlinear numerical methods [32,33] will be extended herein to predict behavior of nonlinear biobased composite laminates. Lin and Hu [34] modeled laminates using the finite element method with bi-linear constitutive models at 0° and 90° and a cubic curve for the shear behavior; the shear contribution to the stiffness matrix was updated with the stress state of the ply. Hashin et al. [35] modeled laminates using a linear model at 0° and nonlinear models in shear and in the transverse direction.

## 3. Mechanical testing of biobased composites

### 3.1. Testing program

The mechanical properties of biobased composite plies are the building block for determining the mechanical properties of laminates and structures made from these materials. Here, eight-layer composite plies were selected to characterize the bulk mechanical properties of plies in laminate structures [36]. Three or more uniaxial tension (0 and 90°), uniaxial compression, shear (conducted as a tension test with 45° fiber orientation), and flexural tests were conducted for each composite material, as summarized in Table 1. Tension, shear and flexural response are reported here and the full body of characterization research can be found in [36]. Fiber volume fractions were determined for each set of specimens and the impact of fiber volume fraction on mechanical properties is discussed. The ply-level tension and shear testing is used in combination with ply orientation, stacking sequence, and component shape to predict the elastic tensile response of three laminate structures using classical laminate plate theory. Ply-level flexural response of the biobased composites are compared with flexural properties of wood-based materials used in building and construction.

### 3.2. Materials and sample preparation

The cellulose acetate plastic matrix is made from 70 wt.% cellulose acetate powder (Sigma Aldrich cellulose acetate, 39.7% acetyl, average Mn 50,000) plasticized by 30 wt.% triethyl citrate 99+%, FCC (Sigma Aldrich). The PHB matrix was made from pellets (Biomer P226), which were a PHB blended with a proprietary citric acid plasticizer. The hemp fabric used in the composites is 100% hemp linen (Hemp Traders, Product CT-L5, 5.8 oz.). The hemp fiber had been water retted then boiled in a solution of sodium hydroxide to remove the lignin from the fiber. The fiber was then combed, spun into yarn, and woven into a fabric. The fabric was further bleached lightly with hydrogen peroxide. The hemp fabric was a plain weave with 45 yarns in the warp direction per 42 yarns in the weft direction.

The plasticized cellulose acetate powder and the PHB pellets were first made into thin films of roughly 25–30 g of material per film using a hot press. The films were then layered with single plies of fabric to form 8-ply composite plates. A pressure of 1.4 MPa was applied for the hemp/CA composites and 0.25 MPa for the hemp/PHB composites. Lower pressure was used for the hemp/PHB composites because the PHB has a lower melt viscosity. Test specimens were cut from the plates using a band saw.

For tensile testing, four dogbone specimens were machined from each plate parallel to the fiber direction being tested, i.e. in the warp (parallel to the roll direction, i.e. 0°) and the weft (perpendicular to the roll direction, i.e. 90°) direction of the fabric. For shear testing, three rectangular specimens of each material were machined from the plates such that the yarns were aligned at 45° angles to the eventual loading direction. For flexural testing, five specimens were machined parallel to the fiber direction (i.e. warp or weft) being tested.

### 3.3. Test methods

All mechanical testing was performed on an MTS 858 table-top tester with a capacity of 14.7 kN. Tensile testing was performed

**Table 1**
Summary of average experimentally determined biocomposite properties.

| Test | Property | Hemp/PHB | Hemp/cellulose acetate |
|---|---|---|---|
| Tensile–warp direction | Number of specimens | 4 | 4 |
| | Volume fraction | 37.9% | 37.1% |
| | Modulus of elasticity (MPa) | 5470 ± 200 | 5430 ± 100 |
| | Maximum strength (MPa) | 55.9 ± 2.6 | 54.4 ± 2.6 |
| | Strain at failure (mm/mm) | 3.50% ± 0.07% | 4.04% ± 0.21% |
| | Poisson's ratio | 0.30 ± 0.05 | 0.30 ± 0.03 |
| Tensile–weft direction | Number of specimens | 4 | 4 |
| | Volume fraction | 39.8% | 40.6% |
| | Modulus of elasticity (MPa) | 3660 ± 150 | 4830 ± 220 |
| | Maximum strength (MPa) | 44.5 ± 1.3 | 54.2 ± 1.0 |
| | Strain at failure (mm/mm) | 9.02% ± 0.47% | 6.41% ± 0.51% |
| | Poisson's ratio | 0.17 ± 0.02 | 0.26 ± 0.03 |
| Shear | Number of specimens | 3 | 3 |
| | Volume fraction | 36.9% | 36.6% |
| | Shear strength (MPa) | 9.85 ± 0.03 | 12.3 ± 0.1 |
| | Shear Modulus (MPa) | 880 ± 10 | 1090 ± 50 |
| Flexure–warp direction | Number of specimens | 5 | 5 |
| | Volume fraction | 40.0% | 42.8% |
| | Ultimate strength (MPa) | 64.8 ± 2.6 | 94.5 ± 3.0 |
| | Flexural modulus (MPa) | 5050 ± 440 | 6560 ± 370 |
| Flexure–weft direction | Number of specimens | 5 | 5 |
| | Volume fraction | 38.9% | 42.8% |
| | Ultimate strength (MPa) | 48.2 ± 0.6 | 80.7 ± 3.5 |
| | Flexural modulus (MPa) | 2770 ± 360 | 5980 ± 670 |

according to ASTM D638 [37] to determine the modulus of elasticity, tensile strength, percent elongation, and Poisson's ratio of the composite materials. The specimens spanned 115 mm between the mechanical wedge grips, which were flat with a saw tooth profile. Transverse and longitudinal strains were measured with strain gages and a 50 mm extensometer, respectively. The tensile load was applied at a constant displacement rate of 5 mm/min. Testing was terminated after failure (tensile rupture) of the specimen. The ultimate stress was taken as the maximum load measured divided by the initial area. The modulus of elasticity was determined from the initial slope (between a point at a strain just above zero and the point at 0.001 mm/mm strain) of the stress–strain response. Poisson's ratio was determined by linear regression of the relation between the transverse and longitudinal strains and applied load.

Shear testing was conducted according to ASTM D3518 [38] to determine in-plane shear modulus, ultimate strength, and ultimate strain. The same mechanical grips as for tensile testing were used, and were separated a distance of 130 mm. As with the tensile tests, tensile load was applied at a constant displacement rate of 5 mm/min and transverse and longitudinal strains were measured with strain gages and a 50 mm extensometer, respectively. While the specimens were tested to failure, the shear strength was controlled by the strength at 5% strain as defined by ASTM D3518 [38] as this value was always reached before rupture.

Flexural tests according to ASTM D790 [39] (three-point flexure) were performed to determine the flexural modulus and strength of the composites. A three-point bending fixture with cylindrical supports with 5 mm radii was secured in the table-top tester. One linear variable displacement transducer was placed at the center of the specimen, directly under the loading nose. The rate of loading was such that the strain rate in the outer tensile fiber of the specimen was 0.1 mm/mm/min. Specimens were loaded and monitored until fiber rupture occurred or in the case of the hemp/PHB in the weft direction until the specimens slipped along the supports. The flexural stress and strain in the outer-most tension fiber were estimated from the experimental results using beam theory and moment–curvature relationships. The flexural modulus was also calculated based on beam theory and was taken as the slope in the linear range of the stress vs. strain plot between a point at a strain just above zero and the point at 0.001 mm/mm strain at the outermost edge in tension. It is noted that neither nonlinear behavior nor differences in compressive and tensile behavior are accounted for in this method. However it is assumed to be a reasonable estimation of material properties for comparison to other reported material properties [36].

Volume fractions were determined according to a modified ASTM D3171 [40], Part I dissolution procedure in which the specified solvents were replaced with acetone and chloroform to dissolve cellulose acetate and PHB, respectively. The solvents were chosen so that they would dissolve the matrix, but not the hemp fabric. The density of the fiber, matrix, and each composite specimen were determined according to ASTM D792 [41] by measuring the mass of the sample and then determining the volume using Archimedes' Principle. Three 10 mm by 50 mm specimens were tested for each composite plate from which mechanical specimens were manufactured.

## 4. Experimental results

### 4.1. Uniaxial tensile response

The uniaxial tensile stress–strain response for each specimen is shown in Fig. 1. Table 1 summarizes the average tensile properties for each biobased composite. The mechanical properties reported are the average and standard deviation of 4 specimens. The stress–strain behavior exhibited by specimens cut from a single plate shows that the material in the plate is consistent, yet greater variation is noticeable near failure because failure likely initiates at flaws in the material that vary between specimens. As will be discussed further below, the bi-linear behavior of specimens tested in the warp direction is attributed to nonlinear behavior of the polymer matrices and the tri-linear behavior of specimens tested in the weft direction was more complex due to a higher yarn crimp. The fiber volume fractions for the specimens varied over a small range from 37.1% to 40.6% suggesting that only slight variation in properties was due to differences in volume fraction.

The failure surface of all specimens was generally perpendicular to the axial direction, with short yarns (<1 mm) protruding from the surface suggesting a failure mode of fiber rupture with slight fiber pull-out. Scanning electron images taken of the fracture surface of the hemp/CA composite (Fig. 2) confirm that while the fibers within the yarn ruptured, the yarns pulled-out from the matrix near the failure surface.

The hemp/CA composites lightened in color within the gage length as they were loaded. This lightening was most likely due to crazing of the matrix; no cracking was visually observed. More significant crazing in the weft direction is attributed to the higher localized strains induced by the larger crimp in the weft direction. In the hemp/PHB composites, tiny, white horizontal cracks, often coinciding with the location of the transverse yarns, were apparent along the length during and after loading. Due to low transverse yarn stiffness and strength, stress concentrations and high localized straining in the matrix likely existed at the transverse fiber surface within the cross-section of the transverse fibers. Thus, the matrix was more likely to fail (crack) here leading to ultimate composite failure at the cracked cross-section.

The composites tested along the warp direction maintained higher strength and stiffness than the composites tested in the weft direction. This was expected because the yarn density was higher in the warp direction (45 yarns in the warp direction for every 42 yarns in the weft direction). Additionally, the crimp angle in the warp direction is expected to be lower than that in the weft direction, leading to higher initial stiffness when loaded in the warp direction. The smaller difference in modulus between the warp and weft for the hemp/CA as compared to difference in modulus in the warp and weft for the hemp/PHB is attributed to the higher manufacturing pressure for the hemp/CA composites that more effectively reduced the crimping in the weft direction.

The hemp/PHB and the hemp/CA behaved in a similar manner in the warp direction, (Fig. 1). While the initial moduli, strength, and Poisson's ratio for the two materials were nearly identical, the hemp/PHB composite had a higher "post-yielding" stiffness and a slightly lower failure strain. The similarities in behavior, given the differences in polymer matrix behavior, suggest that the hemp fabric contributes more strongly to the stress–strain behavior than the matrix material when loaded in the warp direction.

In the weft direction, the hemp/CA composites had a higher ultimate strength, modulus of elasticity, and a lower ultimate strain than the hemp/PHB composites. These differences are attributed to the matrix behavior and the fiber–matrix interfacial behavior and are predominantly a result of the crimping of the hemp fabric in the weft direction. The pure CA matrix is reported to have a higher initial modulus of elasticity over a larger strain range than the PHB polymer [e.g., 42–44]). Like the pure matrices, the hemp/CA composite maintains the initial stiffness, while the stiffness of the hemp/PHB composite degrades almost immediately in tension. The longer plateau region for the hemp/PHB composite is attributed to the lower pressure used to manufacture the hemp/HPB composites. As a result of lower pressure, less crimping of the fabric was removed leading to more deformation and matrix damage as the crimping was stretched in tension. Ultimate failure is hypothesized to have occurred at a lower strength for hemp/PHB

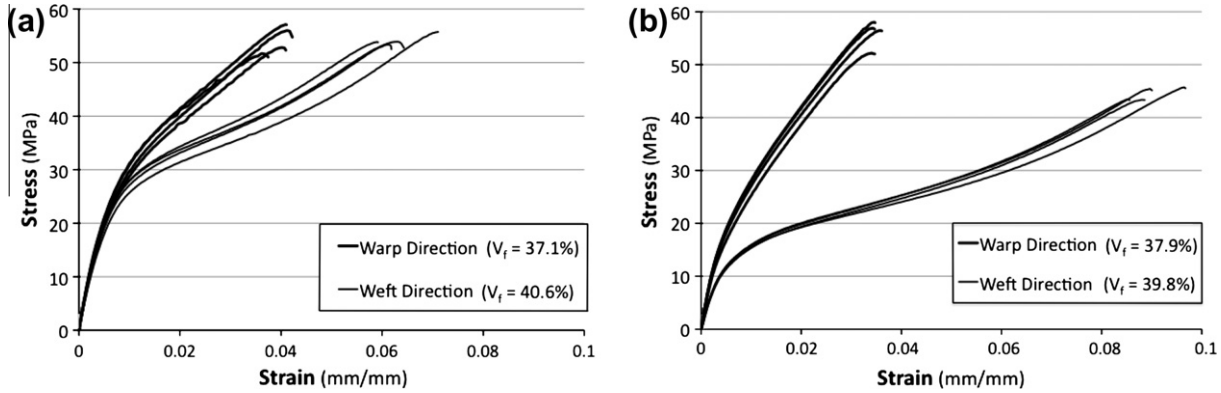


**Fig. 1.** Tensile stress–strain response for (a) hemp/cellulose acetate, and (b) hemp/PHB composites.

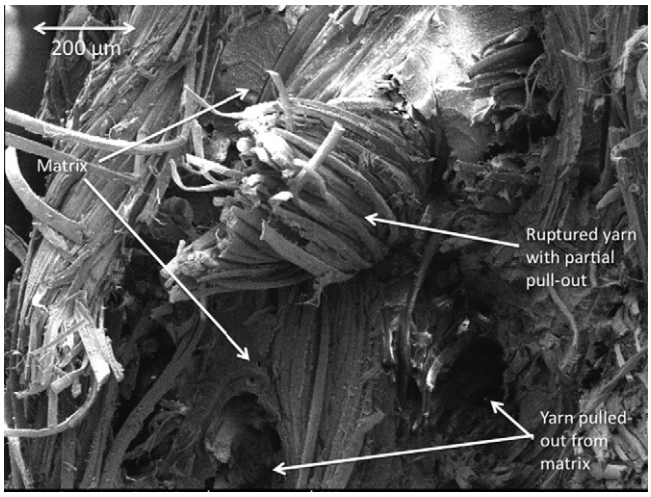


**Fig. 2.** Scanning electron image of hemp/cellulose acetate failure surface.

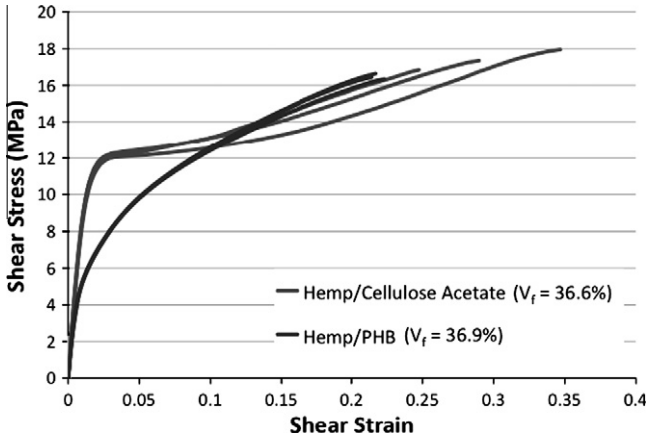


**Fig. 3.** Shear stress–strain response of hemp/cellulose acetate and hemp/PHB composites.

because of stress concentrations in the longitudinal yarns caused by the brittle PHB matrix cracking.

Poisson's ratio in the warp direction was found to be the same (0.30) for both materials. In the weft direction Poisson's ratio was 0.26 for the hemp/CA and 0.17 for the hemp/PHB. From Hooke's Law for orthotropic materials, Poisson's ratio when tested in the weft direction, $v_{21}$, is related to Poisson's ratio when tested in the warp direction, $v_{21}$, by the ratio of the moduli in each direction, $E_1$ and $E_2$. Because the moduli in the weft direction, $E_2$, were smaller than in the warp direction, $E_1$, Poisson's ratio in the weft direction is expected to be lower than in the warp direction, as observed here. Furthermore, because the modulus in the weft direction was lower for the hemp/PHB than for the hemp/CA, but both materials had similar warp direction moduli, Poisson's ratio in the weft direction for the hemp/PHB is expected to be lower than that for the hemp/CA as also was observed here.

The failure strain in the warp direction was relatively similar for the two materials (4.04% for hemp/CA and 3.50% for hemp/PHB) due to similarities in fiber volume fraction in the warp direction and failure by fiber rupture. The failure strains in the weft direction were higher than in the warp direction. The lower volume fraction of fiber in the weft direction produced a lower stiffness resulting in a higher strain at failure. Straightening of the crimp in the weft direction caused significant straining in the matrices resulting in crazing or cracking with little increase in stress. The failure strain for the hemp/PHB in the weft direction was much higher than that for the hemp/CA that is attributed to the flattened fabric and lowered crimping from manufacturing at a higher pressure for the hemp/CA.

### 4.2. Shear response

The shear stress–strain behavior for both hemp/PHB and hemp/CA composites is shown in Fig. 3. The mechanical properties of shear strength and shear modulus are shown in Table 1. As mentioned previously, the maximum strength was taken as the shear stress at 5% strain.

The hemp/CA composite had a higher shear strength and shear modulus than the hemp/PHB composite and maintained initial stiffness significantly longer than the hemp/PHB composite. These responses are similar to the pure matrix response reported for CA [42,43] and PHB [44] in tension, indicating that the matrix behavior impacts the shear behavior more significantly than fiber behavior, as expected due to the fiber orientation. After yielding, the hemp/CA composite response had almost no stiffness, while the hemp/PHB composite maintained a higher stiffness at the higher strains. Both composites gained stiffness beyond 5% strain as a result of fiber reorientation. The orientation of the fibers rotates 1° for every 3.5% shear strain, such that at 20% shear strain, the angle of the yarns would be less than 40°. The realignment of fibers causes an increase in strength at these higher strains.

Both materials failed by fiber rupture at relatively similar strengths. At the higher strains (>5%), significant necking in both materials was observed along with discoloration due to crazing for CA and due to matrix cracking in the PHB. The hemp/PHB failed at a lower strain than the hemp/CA likely because PHB cracks at a lower strain than the CA begins to craze, resulting in earlier full loading of the fibers.

### 4.3. Flexural response

The stress–strain response of the composites tested in flexure with the warp direction in tension and compression is shown in Fig. 4. The flexural properties determined from the load-displacement results are summarized in Table 1. The flexural strength and modulus of elasticity of the hemp/CA composite were greater than those of the hemp/PHB composite. Given the similarities in the tensile properties when tested in the warp direction, the difference in flexural properties is attributed to the stiffer and stronger behavior of the hemp/CA composite in compression, which was observed and reported in Christian and Billington [36]. While the fiber volume fraction for the hemp/CA composite was higher than that for the hemp/PHB composite (Table 1), the magnitude of the difference in strength and stiffness properties was so great that it cannot be fully attributed to the difference in volume fraction.

All specimens that failed did so by tensile rupture at a single (crack) location at mid-span, where the loading was applied. Prior to failure, the hemp/CA composite experienced crazing of the matrix, discoloring from brown to white, around the failure surface at mid-span. Similar to the tensile specimens, the hemp/PHB composites exhibited multiple cracking, in this case at mid-span.

### 4.4. Impact of volume fraction on tensile properties

The relationship between the fiber volume fraction and the tensile properties of modulus of elasticity and strength for the hemp/cellulose acetate composites are shown in Fig. 5. For fiber volume fractions between 30% and 50%, the modulus of elasticity and ultimate strength are positively correlated to the fiber volume fraction, as expected (see for example [17,18]). Considering the $R^2$-values from linear regressions, a stronger relationship exists between the modulus of elasticity and the fiber volume fraction than the strength and the fiber volume fraction. The matrix and fibers tend to behave in parallel (i.e. better bond) in the elastic range, which is consistent with a linear relationship, while cracking of the matrix and failure of the fiber/matrix interface exemplified by pull-out cause the matrix and fiber to act in series near failure. Additionally, failure depends not only on the volume fraction of fibers, but on the strength of the fiber/matrix interface, the percentage of threads in a yarn that are resisting axial load, the friction stresses between threads in a yarn, and imperfections in the material. Thus, it was not expected that strength would be strongly correlated with the fiber volume fraction.

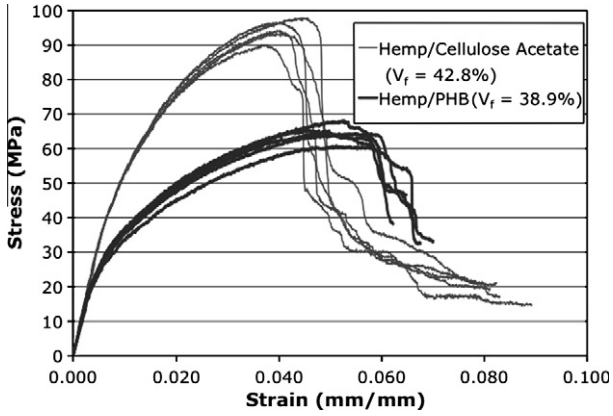


**Fig. 4.** Flexural stress–strain response of hemp/cellulose acetate and hemp/PHB composites.

## 5. Comparison to properties of wood and engineered wood

Of the many materials used in construction, biobased composite materials have properties most similar to wood and engineered wood products. A comparison is briefly presented here, focusing on properties of wood commonly used in construction, namely Douglas Fir (coastal), Western Hemlock, and Ponderosa Pine. Property comparisons are given for wood tested at 12% moisture content as reported by [45] unless otherwise noted. Comparisons are also made to the engineered wood products plywood, oriented strand board (OSB) and glue laminated timber (glulam).

### 5.1. Wood used in construction

In flexure and shear, the biobased composite materials tested here are comparable to wood used in construction (example comparisons given in Table 2). In tension, biobased composites have strengths 4–5 times higher than wood loaded perpendicular to the grain and strengths comparable to wood loaded parallel to the grain. The flexural modulus of the biobased composites is roughly half that of wood parallel to grain. While not reported here, the flexural modulus of wood perpendicular to grain is about 11–35 times less than that reported parallel to grain [46]. Thus, while the wood examples given in Table 2 are stronger and stiffer than the biobased composites in one direction, the fabric-reinforced biobased composites have a more balanced bi-directional strength and stiffness, as expected.

For design, wood properties must be adjusted to account for defects, moisture if clear wood properties are measured, variation in density, and grain slope typical in structural lumber. In addition,

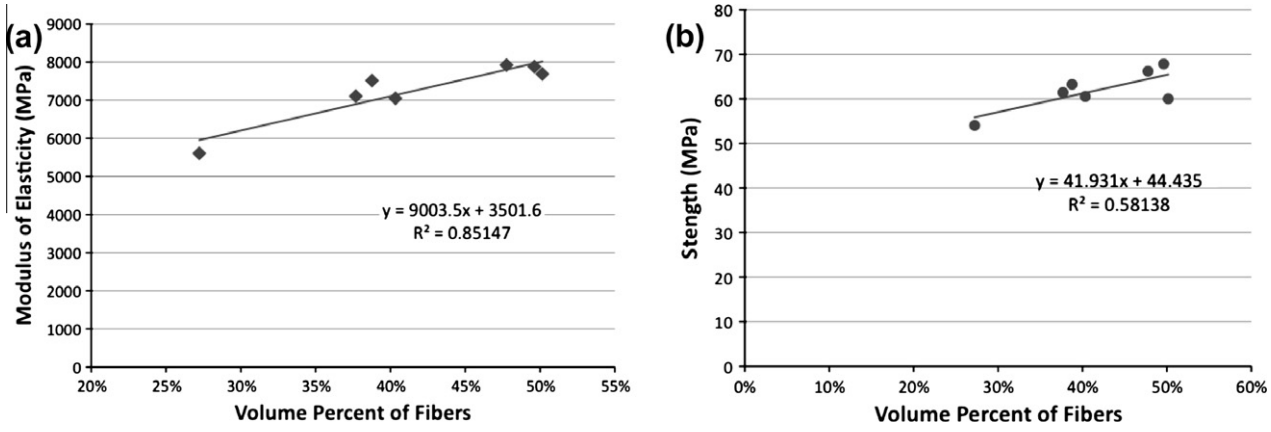


**Fig. 5.** Impact of fiber volume fraction on (a) tensile stiffness and (b) tensile strength.

**Table 2**
Mechanical properties of biocomposites, wood, and engineered wood products.

| Material | Tensile strength (MPa) | Tensile modulus (GPa) | Shear strength (MPa) | Flexural strength (MPa) | Flexural modulus (GPa) | Density (kg/m$^3$) |
|---|---|---|---|---|---|---|
| Hemp/CA | 54 | 5.4 | 12 | 95 | 6.6 | 1300–1370 |
| Hemp/PHB | 56 | 5.5 | 10 | 65 | 6.5 | 1270–1310 |
| Douglas-Fir (coast) [50] | – | – | 7.8 | 85 | 13.4 | 480 |
| Western Hemlock [50] | – | – | 8.6 | 78 | 11.3 | 450 |
| Ponderosa Pine [50] | – | – | 7.8 | 65 | 8.9 | 400 |
| Plywood (B–B Class 1) [46,48] | 27 | 10.3 | 1 | 27 | 10.3[a] | 400–810 |
| Oriented strand board [48,51] | – | – | 1.2 | 21.2 | 5.25 | 490–810 |
| Glulam [50,52] | – | – | – | 26–72 | 10.6 | 320–720 |

[a] Modulus for ply parallel to grain.

clear wood mechanical properties exhibit large coefficients of variation [45]. Given the large variation in properties, the design values are set near the minimum strength and near the average stiffness for the population of lumber. Table 3 compares the biobased composite properties with the allowable mechanical properties most used for design with the wood types considered here after taking into account strength ratios, quality factors, and adjustment factors [36] as per ASTM D245 [47]. In general, the flexural and shear strengths of the biobased composites are expected to be higher than the allowable wood design strengths, and the modulus of elasticity of the biobased composites will remain somewhat lower. For use in nonstructural and structural components, where the actual stiffness is a combination of the modulus of elasticity, $E$, and the moment of inertia, $I$, biobased composite properties comparable to lumber can be achieved by increasing the moment of inertia. An advantage of biobased composites over wood is that biobased composites can easily be molded into structural shapes, including hollow sections. Using less material in the cross-section to achieve higher structural stiffness will also lighten the structure, as the biobased composite densities (1270–1370 kg/m$^3$) are greater than typical densities of wood (320–720 kg/m$^3$) [45].

### 5.2. Engineered wood products

The mechanical properties for plywood, OSB, and glulam are compared to biobased composites in Table 2. The properties of the studied biobased composites are comparable to or better than the properties measured for the engineered wood products in all cases with the exception of the flexural modulus of glulam. It is noted that the modulus of the plywood is for a ply parallel to grain, but when the plies are laminated, some of the plies will be loaded perpendicular to grain which has a modulus that is 35 times smaller than parallel to grain. Therefore the modulus of the biobased composites is likely greater than that for plywood. This brief comparison suggests that biobased composites should be able to directly replace engineered wood products of the same size. However it is also noted that the densities of the biobased composite materials are significantly greater than those for the engineered wood products, which vary from 320–810 kg/m$^3$ [48]. To be an easy-to-implement replacement for engineered wood products, these biobased composites must be engineered to be lighter weight.

## 6. Predicting the mechanical response of biobased laminates

Most models used to predict laminate behavior are based upon laminate plate theory, which predicts the stress–strain behavior for laminates given the engineering constants for each ply, namely $E_1$, $E_2$, $v$ and $G$. The applicability of laminate plate theory to predict the elastic stiffness as well as the nonlinear response of biobased composites using measured ply-level properties is evaluated here. The two modeling approaches used are classical laminate plate theory and a modified laminate plate theory for non-linear

**Table 3**
Allowable design properties for example woods used in construction.

| | Material | Flexural modulus of rupture (MPa) | Flexural modulus of elasticity (MPa) | Shear strength (MPa) |
|---|---|---|---|---|
| Clear green properties | Douglas-Fir (coast) | 53 | 10,800 | 6.2 |
| | Western Hemlock | 46 | 9000 | 5.9 |
| | Ponderosa Pine | 35 | 6900 | 4.8 |
| Strength ratio/quality factor | All wood | 4%–98% | 80%–100% | – |
| Adjustment factor | Softwood | 2.1 | 0.94 | 2.1 |
| Properties adjusted for defects | Douglas-Fir (coast) | 2.1–51.9 | 8640–10,800 | 6.3 |
| | Western Hemlock | 1.9–41.2 | 7200–9000 | 5.9 |
| | Ponderosa Pine | 1.5–34.2 | 5520–6900 | 4.8 |
| Allowable properties | Douglas-Fir (coast) | 1.0–24.7 | 9190–11,490 | 3.0 |
| | Western Hemlock | 0.9–21.5 | 7660–9575 | 2.8 |
| | Ponderosa Pine | 0.7–16.3 | 5870–7340 | 2.3 |
| Biocomposite properties | Hemp/CA | 95 | 6560 | 12.3 |
| | Hemp/PHB | 65 | 5050 | 9.9 |

**Table 4**
Laminate plate specimen description and engineering constants from ply level testing used in laminate plate model.

| Laminate name | Lay-up | Thickness (mm) | Width (mm) | Volume fraction | $E_1$ (MPa) | $E_2$ (MPa) | $v_{12}$ | $G_{12}$ (MPa) |
|---|---|---|---|---|---|---|---|---|
| Laminate 1T | $[0_6/\pm45/0_6]$ | 7.166 | 24.82 | 37.1% | 7600 | 7560 | 0.27 | 1260 |
| Laminate 2T | $[30/-30/60/-60/0]_{sym}$ | 3.942 | 19.96 | 35.8% | 5800 | 4690 | 0.30 | 990 |
| Laminate 3T | $[0_2/45_2/-45_2/90_2]_{sym}$ | 5.585 | 19.12 | 34.9% | 5800 | 4690 | 0.30 | 990 |

**Table 5**
Laminate plate experimental response compared to model predictions.

| Laminate lay-up | | [0/±45/0] | $[30/-30/60/-60/0]_{sym}$ | $[0_2/45_2/-45_2/90]_{sym}$ |
|---|---|---|---|---|
| Volume fraction | | 37.1% | 35.8% | 34.9% |
| Modulus (MPa) | Measured | 6820 ± 290 | 4770 ± 60 | 4410 ± 210 |
| | CLPT predicted (% dif.) | 7380 (8%) | 4170 (13%) | 4090 (7%) |
| | NLPT predicted (% dif.) | 6760 (1%) | 4820 (2%) | 4300 (3%) |
| Strength (MPa) | Measured | 58.5 ± 0.8 | 40.9 ± 1.9 | 42.0 ± 2.5 |
| | NLPT predicted (% dif.) | 63.9 ($\varepsilon$ = 0.025) (9%) | 50.4 ($\varepsilon$ = 0.032) (23%) | 51.4 ($\varepsilon$ = 0.038) (22%) |

materials. Three hemp/cellulose acetate composite laminates were designed (Table 4) and their tensile response predicted. The specimens of each laminate design were then fabricated and tested using the same test procedure and set up as used for the tension specimens described above, and the validity of the models was evaluated.

For predicting the elastic modulus of the laminates in uniaxial tension, classical laminate plate theory (CLPT) was used with the engineering constants given in Table 4. Laminate 1T was manufactured from 100% hemp linen, 5.8 oz. purchased from Hemp Traders in June 2007. Laminates 2T and 3T were manufactured from 100% hemp linen, 5.8 oz. purchased from Hemp Traders in June 2008. Because the properties of hemp vary greatly depending on the environmental conditions during growth the mechanical properties of the fabric purchased at different times, although bearing the same name, were different. Thus, the ply properties used in the laminate models were different depending on the hemp used.

To predict the nonlinear response of the laminates in uniaxial tension, a simple non-linear modeling method that uses CLPT as its basis was investigated. In the nonlinear model, displacement is applied incrementally and the laminate stiffness matrix is updated after each increment using stiffness measurements from the ply-level experiments. The Euler, or simple-step, method is used wherein the strain in the direction of loading is applied to the model in small increments, and post-peak behavior can be captured. After a strain increment is applied, the applied force and the internal strains are calculated. Given the internal strains in each ply, the moduli for each ply, the tangent moduli corresponding to the initial strain at the beginning of the increment, and ultimately the laminate stiffness matrix are updated, and the next increment of strain is applied. The analysis continues until the maximum strain of any ply is reached, as defined by the experimental ply data. For these analyses, all forces except for the force in the loading direction are set to zero.

The nonlinear constitutive model for the material was developed by discretizing the stress–strain curves from the ply-level experimental testing into linear segments (each relating to a strain range of 0.001 mm/mm in size) over which the moduli are assumed constant [32]. Increases in the segment size resulted in predictions of stresses considerably higher than those actually occurring. Uncoupled stress–strain behavior for each strain component was assumed so as to use the uniaxial stress–strain data directly [32,33]. Therefore, in this simple model, each moduli depends only on the magnitude of the related strain experienced.

The predicted and experimental results of the three laminate designs are presented in Table 5 and Fig. 6. CLPT predicted the initial stress–strain response well, predicting the initial moduli of all three laminate designs within 7–13%. This result indicates that there is likely no interfacial debonding between the plies of these laminates. As expected, upon laminate yielding the stress–strain response predicted by the model and that measured experimentally diverged, thus CLPT is only useful in predicting the initial stiffness of the hemp/cellulose acetate composites.

The nonlinear model is more accurate in predicting the stiffness of the laminates (within 1–2% difference) but it overestimates the strength of the laminates by 9–23%. This overestimation of strength is attributed to the assumption of uncoupled stress–strain for each strain component in the constitutive model. If the strains

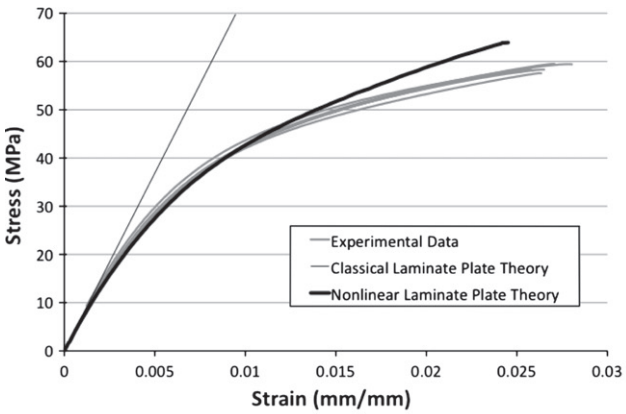


(a) Laminate 1T $[0_6/\pm45_6/0_6]$

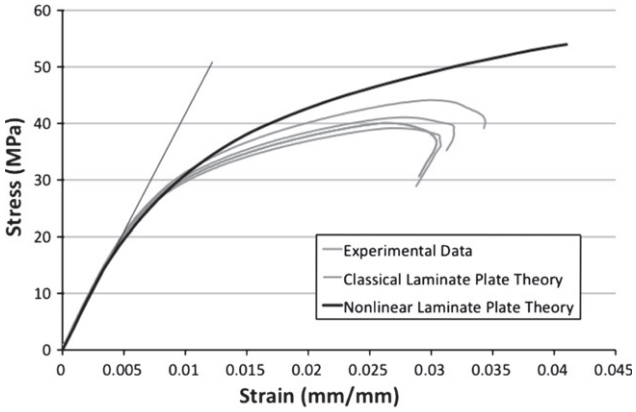


(b) Laminate 2T $[30/-30/60/-60/0]_{sym}$

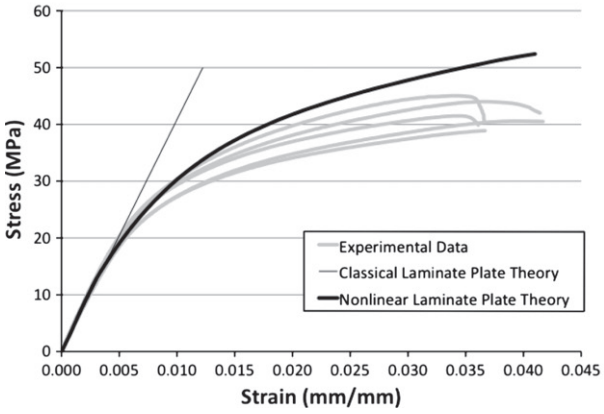


(c) Laminate 3T $[0_2/45_2/-45_2/90_2]_{sym}$

**Fig. 6.** Comparison of laminate plate theory models to experimental behavior of laminates in tension.

were coupled, as it is in reality, the stiffness and strength would be expected to degrade more quickly.

For designs in which deflection limits the design, which is likely for the biobased composites studied here, CLPT provides a stiffness prediction that is relatively accurate with less effort than the nonlinear model. However, because the biobased composites behave in a non-linear fashion at low strains (and stresses), either very large cross-sections would be required to keep stresses low and maintain linear behavior or the design method would need to account for nonlinear behavior. The simple nonlinear model evaluated here demonstrates that while reasonable predictions can be made, more advanced modeling is necessary to predict the true nonlinear response. An example model with applicability to these materials is given in Michel & Billington [49].

Significantly different mechanical properties measured for the composite laminates made from different batches of hemp fabric with the same nominal fabric architecture suggest that variations in the natural fibers from different environmental conditions during growth and variations in yarn and fabric processing and architecture can significantly affect the biobased composite behavior. Thus, further investigation is needed to understand these variations, and high resistance and safety factors likely will be required by design codes for biobased composite components to account for variations in fabric properties between batches of natural fabric.

## 7. Conclusions

Mechanical property testing of hemp/cellulose acetate and hemp/PHB biobased composite materials was conducted to evaluate their potential for replacing wood and engineered wood products in the construction industry as well as the ability of well-established laminate plate theory models to predict their stiffness and nonlinear response.

The composites exhibit a bilinear response in uniaxial tension when loaded in the warp direction of the fiber, which is attributed to nonlinear behavior of the polymer matrices. When loaded in the weft direction a tri-linear response is observed due to nonlinear polymer behavior as well as extension of the yarn crimp, which is higher in the weft direction than the warp direction. Higher ductility was observed in the hemp/PHB composites due to lower pressure used during manufacturing (limiting the amount of crimp removed), which was necessary due to the lower melt viscosity of the PHB compared with the CA matrix. The failure surface of all specimens was generally perpendicular to the direction of loading, with short yarns (<1 mm) protruding from the surface suggesting a failure mode of fiber rupture with slight fiber pull-out.

The differences in shear response of the composites reflected the differences reported for the plain polymer matrices in tension as expected. In flexure, the hemp/CA composites exhibited higher stiffness, which is attributed to higher stiffness in compression. Failure by fiber rupture similar to uniaxial tension was observed in both composites.

For fiber volume fractions between 30% and 50% in the hemp/cellulose acetate composites, the modulus of elasticity and ultimate strength are positively correlated to the fiber volume fraction. A stronger relationship was apparent between the modulus of elasticity and the fiber volume fraction than the strength and the fiber volume fraction, which is attributed to the assumption that fiber and matrix behave in parallel which is true in the elastic range but not near failure and to the additional parameters that contribute failure, such as strength of fiber/matrix interface and friction between threads of the yarn.

Both biobased composite materials studied here exhibited strengths in flexure and shear comparable to the strengths of the wood and wood-based products used in construction considered here. The tensile strength of the biobased composites was lower than the wood strength parallel to the grain and higher than the wood strength perpendicular to the grain. The biobased composite moduli of elasticity were between 35% and 75% of the wood moduli parallel to grain. In general, the strengths of the biobased composites are expected to be higher and the moduli of elasticity are expected to be lower than the allowable wood design strengths and moduli. While structural shape could be manipulated to achieve a comparable stiffness using the biobased composites to replace the types of wood compared here, the biobased composites may be directly used in place of engineered-wood products such as furniture, crates, pallets, shelves, and formwork due to their similar properties. However the higher densities of the biobased composites studied here as compared to both wood and engineered-wood products may limit their implementation in construction and efforts to develop lightweight biobased composites are needed.

Classical laminate plate theory was shown to be effective in predicting the initial linear behavior of three laminate designs subjected to uniaxial tension. Use of this model would be appropriate for design of deflection-limited applications within certain stress ranges. A modified nonlinear laminate plate theory model predicts the initial stress–strain response well and overestimates the strength by 9–23%, which is attributed to using uncoupled stress–strain response for each strain component. Accurate ultimate strain predictions would require the model to capture the more complex behavior near failure, including behavior at the fiber/matrix interface, interaction between threads in a yarn, cracking of the matrix and the effects of irregularities in the composite. While the simple models provided an adequate prediction of laminate behavior at low strains, to predict nonlinear behavior at higher strains, it is recommended to use nonlinear constitutive models in finite element analyses to predict the response, which is asymmetric in tension and compression as well as in the orthotropic directions.

## Acknowledgements

This research was funded in part by the Woods Institute for the Environment at Stanford University as well as the California EPA (Grant No. 07T3451). The first author was supported by a National Science Foundation Graduate Research Fellowship. The opinions expressed in this paper are those of the authors and do not necessarily represent the opinions of any of the sponsors.

## References

[1] EPA. Estimating 2003 building-related construction and demolition materials amounts. US Environmental Protection Agency Report #: EPA530-R-09-002. March; 2009.
[2] Sandler K. Analyzing what's recyclable in C&D debris. Biocycle 2003:51–4.
[3] Mohanty AK, Misra M, Drzal LT, editors. Natural fibers, biopolymers, and biobased composites. Boca Raton (FL): CRC Press, Taylor & Francis Group; 2005.
[4] Wool RP, Sun XS, editors. Bio-based polymers and composites. Amsterdam: Elsevier, Inc.; 2005.
[5] John MJ, Thomas S. Biofibres and biobased composites. Carbohydr Polym 2008;71:343–64.
[6] Riedel U, Nickel J. Natural fibre-reinforced biopolymers as construction materials. Die Angew Makromol Chem 1999;272:34–40.
[7] Netravali A, Chabba S. Composites get greener. Mater Today 2003;April:24–31.
[8] Dweib MA, Hu B, O'Donnell A, Shenton HW, Wool RP. All natural composite sandwich beam for structural applications. Compos Struct 2004;63:147–57.
[9] Hu B, Dweib M, Wool RP, Shenton HW. Bio-based composite roof for residential construction. J Archit Eng 2007;13(3):136–43.
[10] Burgueño R, Quagliata MJ, Mehta GM, Mohanty AK, Misra M, Drzal LT. Sustainable cellular biobased composites from natural fibers and unsaturated polyester resin for housing panel applications. J Polym Environ 2005;13(2):139–49.
[11] Burgueño R, Quagliata MJ, Mohanty AK, Mehta GM, Drzal LT, Misra M. Hierarchical cellular designs for load-bearing biobased composites beams and plates. Mater Sci Eng A 2005;390:178–87.
[12] Van de Velde K, Kiekens P. Biopolymers: overview of several properties and consequences on their applications. Polym Test 2002;21:433–42.

[13] Lackey E, Vaughan, JG, Inamdar K, Hancock B. Statistical characterization of pultruded composites with natural fiber reinforcements. Composites 2004 convention and trade show. American Composites Manufacturers Association: Tampa, Florida; 2004.
[14] Singh B, Gupta M. Natural fiber composites for building application. In: Mohanty AK, Misra M, Drzal LT, editors. Natural fibers, biopolymers, and biobased composites. Boca Raton (FL): CRC Press, Taylor & Francis Group; 2005a. p. 261–90.
[15] Singh B, Gupta M. Performance of pultruded jute fibre reinforced phenolic composites as building materials for door frames. J Polym Environ 2005;13(2):127–37.
[16] Choi JS, Lim ST, Choi HJ, Hong SM, Mohanty AK, Drzal LT, et al. Rheological, thermal, and morphological characteristics of plasticized cellulose acetate composites with natural fiber. Macromol Symp 2005;224:297–307.
[17] Mohanty AK, Wibowo A, Misra M, Drzal LT. Effect of process engineering on the performance of natural fiber reinforced cellulose acetate biobased composites. Composites Part A 2004;35:363–70.
[18] Taha I, Ziegmann G. A comparison of mechanical properties of natural fiber filled biodegradable and polyolefin polymers. J Compos Mater 2006;40(21):1933–46.
[19] Keller A. Compounding and mechanical properties of biodegradable hemp fibre composites. Compos Sci Technol 2003;63:1307–16.
[20] Bodros E, Pillin I, Montrelay N, Baley C. Could biopolymers reinforced by randomly scattered flax fibre be used in structural applications? Compos Sci Technol 2007;67(3–4):462–70.
[21] Wong S, Shanks R, Hodzik A. Properties of poly(3-hydroxyburic Acid) composites with flax fibres modified by plasticizer absorption. Macromol Mater Eng 2002;287:647–55.
[22] Lee SG, Choi SS, Park WH, Cho D. Characterization of surface modified flax fibers and their biobased composites with PHB. Macromol Symp 2003;197:89–99.
[23] Mohanty AK, Khan MA, Sahoo S, Hinrichsen G. Effect of chemical modification on the performance of biodegradable jute–yarn/biopol composites. J Mater Sci 2000;35:2589–95.
[24] Khan MA, Ali KMI. Study on physical and mechanical properties of biopol–jute composites. Polym–Plast Technol Eng 1999;38(1):99–112.
[25] Singh S, Mohanty AK, Sugie T, Takai Y, Hamada H. Renewable resource based biobased composites from natural fiber and polyhydroxybutyrate-co-valerate (PHBV) bioplastic. Composites Part A 2008;39:875–86.
[26] Shibata M, Takachiyo K-I, Ozawa K, Yosomiya R, Takeishi H. Biodegradable polyester composites reinforced with short abaca fiber. J Appl Polym Sci 2002;85(1):129–38.
[27] Luo S, Netravali AN. Interfacial and mechanical properties of environment-friendly "green" composites made from pineapple fibers and poly(hydroxybutyrate-co-valerate) resin. J Mater Sci 1999;34(15):3709–19.
[28] Chabba S, Netravali AN. 'Green' composites Part 1: Characterization of flax fabric and glutaraldehyde modified soy protein concentrate composites. J Mater Sci 2005;40:6263–73.
[29] Mohanty AK, Khan MA, Hinrichsen G. Influence of chemical surface modification on the properties of biodegradable jute fabrics–polyester amide composites. Composites Part A 2000;31:143–50.
[30] Burgueño R, Quagliata M, Mohanty AK, Mehta G, Drzal LT, Misra M. Load-bearing natural fiber composite cellular beams and panels. Composites Part A 2004;35:645–56.
[31] Isaac C. Parametric material layout optimization of natural fiber composite panels. Master of Science Thesis. Michigan State University; 2005.
[32] Amijima S, Adachi T. Nonlinear stress–strain response of laminate composites. J Compos Mater 1979;13:206–18.
[33] Kuppusamy T, Nanda A, Reddy JN. Materially nonlinear analysis of laminated composite plates. Compos Struct 1984;2:315–28.
[34] Lin W-P, Hu H-T. Nonlinear analysis of fiber-reinforced composite laminates subjected to uniaxial tensile load. J Compos Mater 2002;36(12):1419–50.
[35] Hashin Z, Bagchi D, Rosen BW. Non-linear behavior of fiber composite laminates. NASA contractor report # CR2313; 1974.
[36] Christian SJ, Billington SL. Mechanical characterization and structural assessment of biocomposites for construction, technical report no. 168, John E. Blume Earthquake Engineering Center, Stanford University; 2009. p. 198.
[37] ASTM D638. ASTM D638-01. standard test method for tensile properties of plastics. Annual book of ASTM standards. America Society for Testing of Materials, PA; 2001.
[38] ASTM D3518. ASTM D3518-07. Standard test method for in-plane shear response of polymer matrix composite materials by tensile test of a ±45° laminate. Annual book of ASTM standards. American Society for Testing of Materials, PA; 2007.
[39] ASTM D790. ASTM D790–07. Standard test methods for flexural properties of unreinforced and reinforced plastics and electrical insulating materials. Annual book of ASTM standards. American Society for Testing of Materials, PA; 2007.
[40] ASTM D3171. ASTM D3171-06. Standard test methods for constituent content of composite materials. Annual book of ASTM standards. American Society for Testing of Materials, PA; 2006.
[41] ASTM D792. ASTM D792-00. Standard test methods for density and specific gravity (relative density) of plastics by displacement. Annual Book of ASTM Standards. PA: American Society for Testing of Materials; 2000.
[42] Ghiya VP, Dave V, Gross RA, McCarthy SP. Plasticization and biodegradation of cellulose acetate. ANTEC 1995:3726–30.
[43] Mohanty AK, Wibowo A, Misra M, Drzal LT. Development of renewable resource-based cellulose acetate bioplastic: effect of process engineering on the performance of cellulosic plastics. Polym Eng Sci 2003;43(5):1151–61.
[44] Biomer. Biomer polyesters; 2011. <http://www.biomer.de> [accessed 21.01.08]
[45] Kretschmann DE. Mechanical properties of wood. wood handbook, Forests Product Laboratory, FPL-GTR-190; 2010. p. 5-1–46 [chapter 5].
[46] Hurd MK. Formwork for concrete. Detroit: American Concrete Institute; 1995.
[47] ASTM D245. ASTM D245-06. Standard practice for establishing structural grades and related allowable properties for visually graded lumber. Annual book of ASTM standards. American Society for Testing of Materials, West Conshohocken, PA; 2006.
[48] APA. Relative Lightness in Weight, APA-The Engineered Wood Association; 2011. http://www.performancepanels.com/index.cfm?content=app_pp_atr_weight [28.01.11]
[49] Michel A, Billington SL. Flexure and shear performance of PHBV/Hemp engineered biobased composite sandwich panels. Composites 2011. Florida (USA): American Composites Manufacturers Association; 2011 (February).
[50] Green DW, Winandy JE, Kretschmann DE. Mechanical properties of Wood. Wood handbook—Wood as an engineering material, Gen. Tech. Rep. FPL–GTR–113. Madison, WI: U.S. Department of Agriculture, Forest Service, Forest Products Laboratory; 1999.
[51] Thomas WH. Concentrated load capacity and stiffness of oriented strand board: Calculation versus test. J Struct Eng 2002;128(7):908–12.
[52] Issa CA, Kmeid Z. Advanced wood engineering: Glulam beams. Constr Build Mater 2005;19(2):99–106.